

Pn-wave observations in Costa Rica

Ronnie Quintero^{1,2} and Ota Kulhánek²

¹ *Observatorio Vulcanológico y Sismológico de Costa Rica, Heredia, Costa Rica.*

² *Department of Earth Sciences, Seismology, Uppsala University, Sweden.*

Received: September 24, 1997; accepted: February 18, 1998.

RESUMEN

Tiempos de arribos, medidos en la Red Sismográfica de Costa Rica, fueron empleados para extraer información sobre la corteza y el manto por debajo de Costa Rica. Datos de tiempos de arribo de la onda P y S de 100 sismos locales y regionales ocurridos durante el período 1984-1990 fueron usados para obtener la velocidad Pn, la razón de Poisson, la anisotropía de la velocidad Pn y la corrección de las estaciones. La razón de Poisson para la capa superior del manto por debajo de Costa Rica es 0.265 y la velocidad de Pn encontrada es de 7.81 km/sec. La presente investigación no muestra variaciones anisotrópicas significantes para la onda Pn. La profundidad del Moho se calcula en 34 km, aproximadamente.

PALABRAS CLAVE: Método de tiempos de arribos, velocidad Pn, razón Vp/Vs, anisotropía, Costa Rica.

ABSTRACT

P- and S-wave arrival-time data from 100 local and regional earthquakes recorded by the OVSICORI-UNA Costa Rica seismographic network, between 1984 to 1990, are employed to extract crustal and upper mantle information beneath Costa Rica. Pn-wave velocity, Poisson's ratio, velocity anisotropy and station corrections were calculated in this study. Poisson's ratio for the uppermost mantle beneath Costa Rica is 0.265 and the Pn velocity is 7.81 km/sec. The present study does not reveal any significant Pn velocity anisotropy. The computed Moho depth beneath Costa Rica is approximately 34 km.

KEY WORDS: Time-term method, travel times, Pn velocity, Vp/Vs ratio, anisotropy, Costa Rica.

INTRODUCTION

Costa Rica is located near the southern terminus of the Middle America Trench (MAT) in a complicated seismotectonic environment. The most prominent feature of this region is the tectonically active junction between four major lithospheric plates, namely the South American, Nazca, Cocos and Caribbean (Mann, 1995). The interaction of these plates generates subduction of the Cocos plate under the Caribbean plate, subduction of seamounts in southern Costa Rica, a volcanic chain, back-arc thrusting and fracture zones (Silver *et al.*, 1995).

We apply the time-term method of Scheidegger and Willmore (1957) for extracting crustal thickness and uppermost mantle velocity from an ensemble of seismic-wave arrival-times. We use P and S waves from local and regional earthquakes that occurred during the period from 1984 to 1990, recorded by the Observatorio Vulcanológico y Sismológico de Costa Rica, Universidad Nacional (OVSICORI-UNA) local network. From this data set we estimate Pn-wave velocity, Pn-velocity anisotropy, Poisson's ratio (Vp/Vs) and station corrections.

Matumoto *et al.*, (1977) carried out a travel-time study and found that the thickness of the crust beneath the central volcanic axis of northern Costa Rica is about 43 km and the upper mantle velocity is 7.9 km/sec. Our results for mantle

velocity are similar, but we obtained a significantly smaller crustal thickness. We discuss this disparity in conclusions.

DATA

The OVSICORI-UNA seismographic network is a telemetered network consisting of 26 seismographic stations. The seismometers are mainly short-period vertical-component Ranger SS-1 (1 Hz) instruments (Güendel *et al.*, 1989). It has been operating since early 1984 and is administered by the Universidad Nacional Autónoma. Location of stations used in this study is displayed in Figure 1 and station coordinates may be found, e.g., in Güendel *et al.* (1989). The principal data gathered by the network, are seismograms from local and regional earthquakes. To determine the Pn velocity, the present study makes use of 100 earthquakes from the time period 1984-1990, with duration magnitude (as defined in OVSICORI, 1993) $M_c \geq 4$, and in the distance range from 116 km to 666 km. Respective epicenters are displayed in Figure 1. Data selection is based on the following criteria. We need at least one station with a Pn-phase reading. The event should be recorded by as many stations as possible, usually more than 6 stations. Focal depths of events considered are less than 45 km. The event location is also reported in the ISC bulletin. We consider only events located by OVSICORI-UNA within location error limits given by ISC. In total, we selected 100 events and made use of measurements at 26 stations. The selected events show root-mean-

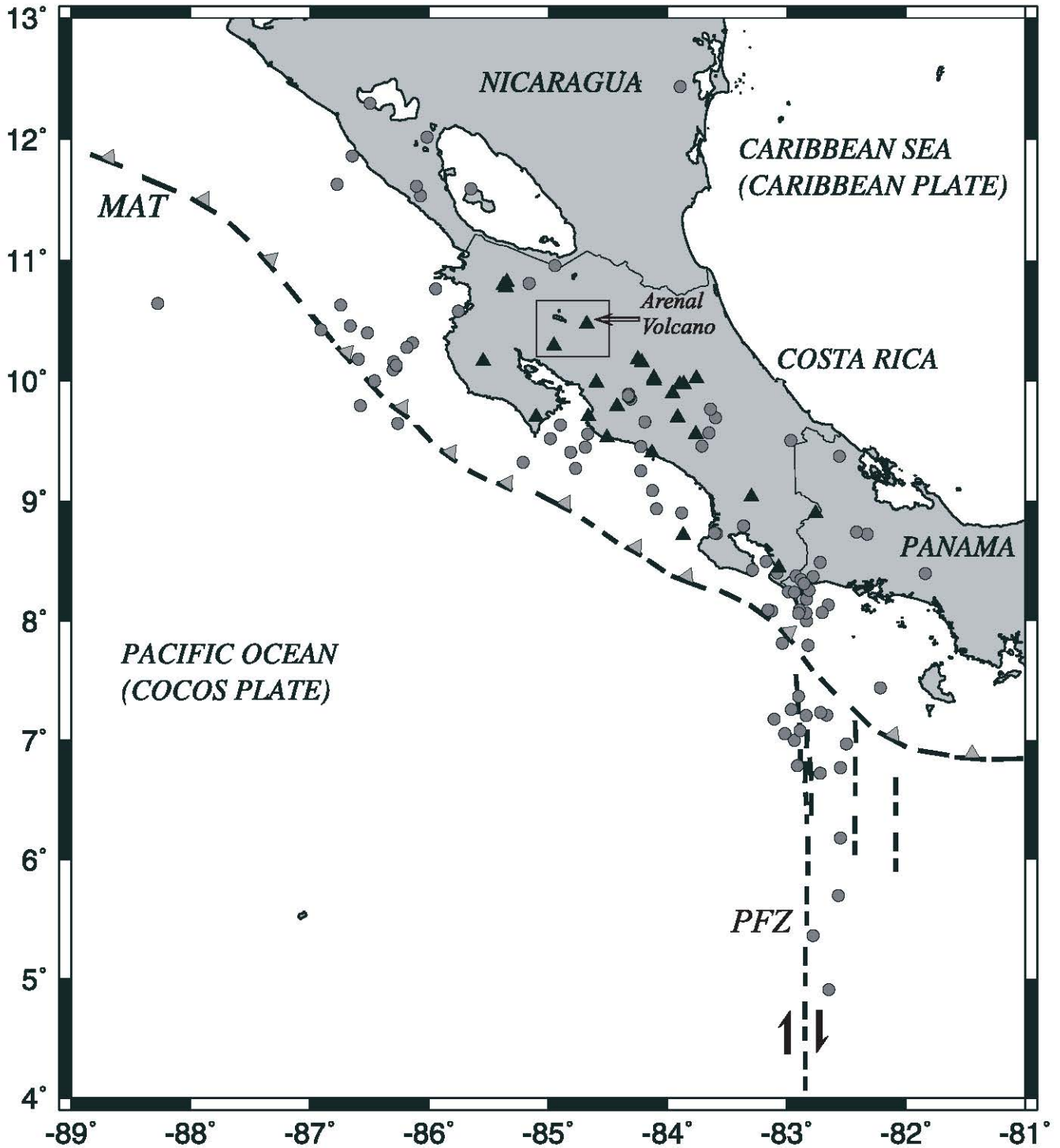


Fig. 1. Location of events used in this study and recorded by the OVSICORI-UNA seismographic network. The epicenters are indicated by circles and the stations by triangles. MAT= Middle America Trench, PFZ= Panama Fracture Zone. The rectangular zone indicates the location of the array used in the work of Matumoto *et al.*, (1977).

square time residuals ($T_{OBS} - T_{CAL}$) less than 0.4 sec, where T_{OBS} refers to OVSICORI-UNA measurements. Due to the elongated configuration of the OVSICORI-UNA network and to the distribution of selected earthquakes, roughly parallel

with the trench, source-to-station azimuths are concentrated around 110° and 325° (see Figure 2).

Arrival-time readings from OVSICORI-UNA seismo-

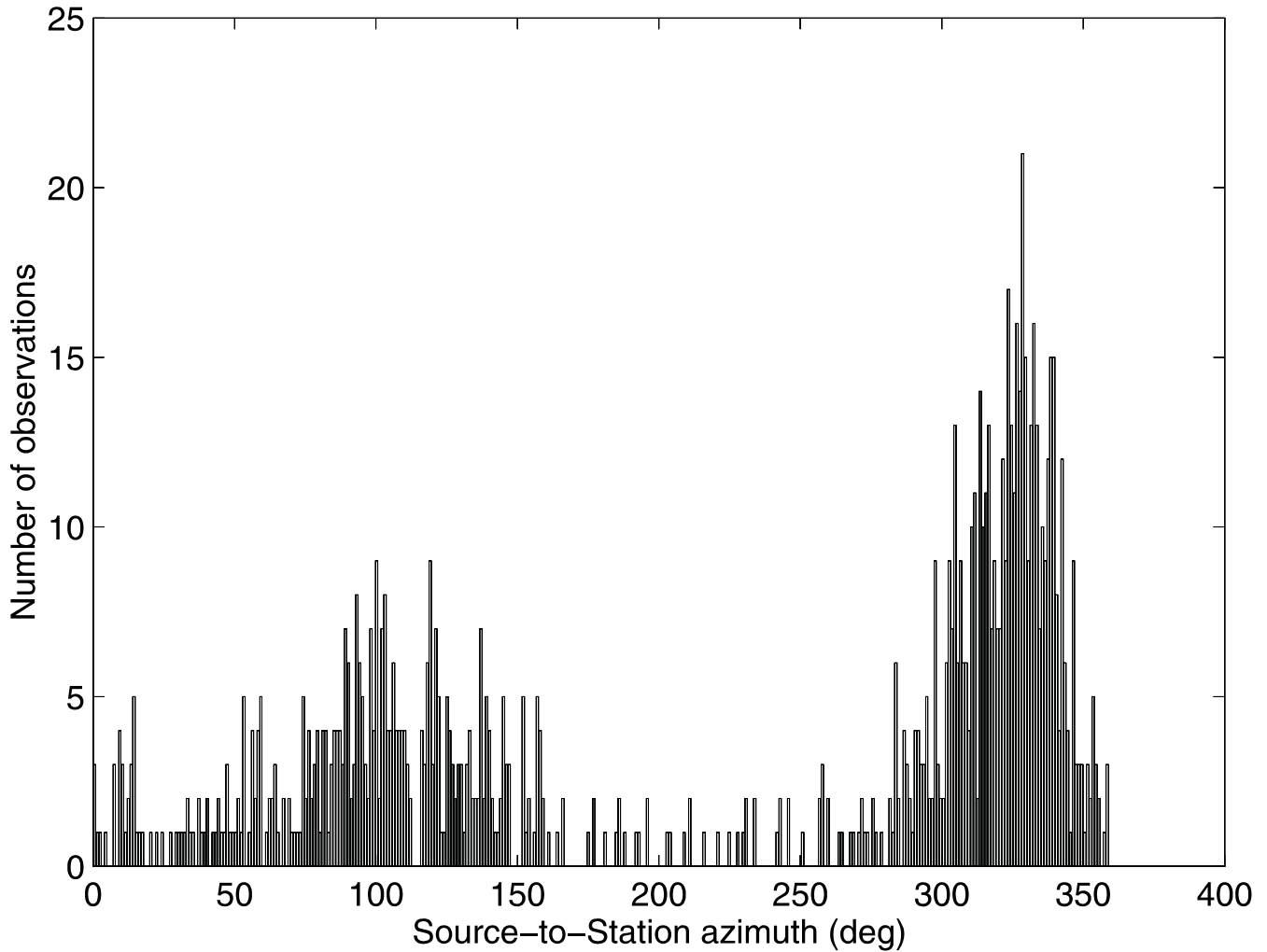


Fig. 2. Histogram of source-to-station azimuths used in this study.

logical bulletins are compiled and classified with respect to the quality of the onsets. For P and S waves, the onsets are classified in the usual way as either “i” (for impetus) or “e” (for emersio) and assigned a relative weight between 0 to 4, depending on the quality of the seismogram, as defined in the program Hypoinverse (Klein, 1984). All earthquakes are located using the program Hypoinverse (Klein, 1984), with the 1D P-velocity model listed in Table 1 (see Güendel, 1986 for the reference model). A V_p/V_s ratio of 1.78 is used in the earthquake-relocation. The hypocenters are concentrated along the Wadati-Benioff zone and around the Panama Fracture Zone (see Figure 1).

TRAVEL-TIME STUDIES

Assuming that locations and origin times of employed earthquakes do not contain large errors, the initial identification of the recorded P or S wave is based upon the 1-D velocity model described in Table 1 and on information provided by ISC. To identify the wave type, we compute the

Table 1

P-velocity model used in the location procedure

Vp km/sec	Depth km
5.10	0.00
6.20	8.20
6.60	21.10
7.80	43.40
8.15	60.00

theoretical travel time for direct and refracted waves and chose the wave type, which gives the minimum difference between the corresponding, observed and calculated travel

time. As shown and discussed below, our depth to Moho is 34 km and differs from that given by Matumoto *et al.* (1977, see also Table 1). However, we do not believe that this ambiguity will influence significantly travel times of direct P waves (for events shallower than 34 km, about 75% of present data) and of Pn for larger distances.

For a general case, where the source is at any arbitrary depth in a model consisting of N layers over a half-space, the corresponding travel time, for a ray refracted along the top of the k-th layer and a source in the j-th layer, becomes

$$T_{jk} = \frac{\Delta}{v_k} - \frac{\zeta \Omega_{kj}}{v_j v_k} + \sum_{i=1}^{j-1} \frac{h_i \Omega_{ki}}{v_i v_k} + 2 \sum_{i=j}^{k-1} \frac{h_i \Omega_{ki}}{v_i v_k} . \quad (1)$$

The corresponding critical distance reads

$$\xi_{jk} = -\frac{\zeta v_j}{\Omega_{kj}} + \sum_{i=1}^{j-1} \frac{h_i v_i}{\Omega_{ki}} + 2 \sum_{i=j}^{k-1} \frac{h_i v_i}{\Omega_{ki}} \quad (2)$$

for $j = 1, 2, \dots, N-1$ and $k = 2, 3, \dots, N$. Δ is the epicentral distance, ζ is the source depth measured from the top of the j-th layer, $\Omega_{ki} = (v_k^2 - v_i^2)^{1/2}$ and $\Omega_{kj} = (v_k^2 - v_j^2)^{1/2}$, h_i is the thickness and v_i the velocity of the i-th layer (Lee and Steward,

1981). In the present work, a structural model specified in Table 1 has been used in the phase identification.

For the refracted wave, and for an accepted location and origin time, we determine the apparent velocity v , from the relation

$$t_i - d_i = d + \Delta_i/v . \quad (3)$$

Where t_i is the travel time to the i-th station, d_i is a delay associated with the i-th station, d is a fixed delay, Δ_i is the epicentral distance and v is the apparent velocity. We solved eqs. (3) for d and v by weighted least-squares. The used weights are associated with the inverse standard deviation of the residuals, and with the quality of the seismograms, as explained before.

A total of 581 recorded onsets, from a distance range between 116 and 666 km, were interpreted as Pn arrivals. The travel time versus distance distribution was fitted with a straight line (Figure 3). The resulting relation reads

$$t = (5.6217 \pm 0.1434) + (0.1284 \pm 0.0005)\Delta . \quad (4)$$

The inverse slope of the straight line in Figure 3 gives a Pn velocity of 7.79 km/s.

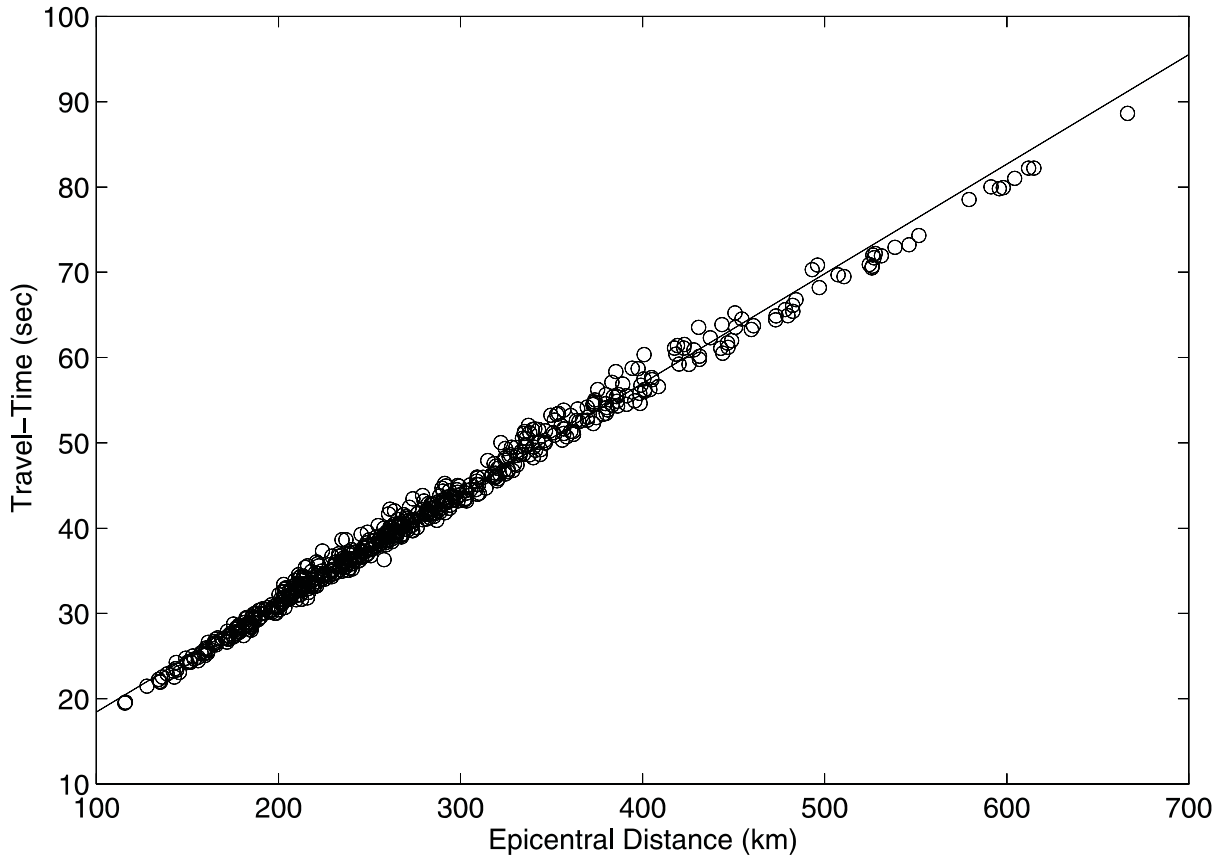


Fig. 3. Travel times of Pn waves plotted against epicentral distances. There are 581 measured travel times in the distance range from 116 km to 666 km used in the diagram.

As can be seen in the plot of the travel-time versus epicentral distance for the Pg wave (Figure 4), we can fit the data for short distances, i.e. approximately between 11 km and 150 km and 0-35 km focal depth, with another straight line. This approximation gives an average Pg velocity of 6.56 km/sec and Moho depth of 34 km. We calculate the depth h_1 to Moho using the equation $t = \Delta/v_2 + 2h_1 (v_2^2 - v_1^2)^{1/2}/v_1v_2$ where the time is given in eq. (4), v_2 is the Pn velocity and v_1 is 6.56 km/sec.

Although the OVSICORI-UNA seismic network consists mainly of vertical-component instruments, we also tried to employ Sn- and Sg-wave arrival-times to estimate the Vp/Vs ratio by constructing the Wadati diagrams. We use the slope in the graph (Ts-Tp) versus Tp, where Ts-Tp is the difference between the S- and P-wave travel-times (Kisslinger and Engdahl, 1973). In order to make use of data from a number of shocks, we adopted travel times rather than arrival times. In our case, 298 observations of Pn- and Sn-wave travel-times give a Vp/Vs value of 1.769 (Figure 5). Then, from the relation between Vp, Vs and σ (isotropic material), we obtain Poisson's ratio, $\sigma = 0.265 \pm 0.001$, for the layer just below Moho.

If we combine direct waves and waves refracted from Moho and other discontinuities, then the Wadati diagram exhibited in Figure 6 provides an average Vp/Vs ratio of 1.777 ± 0.002 , and Poisson's ratio of $\sigma = 0.268 \pm 0.001$. Differences between the Vp/Vs ratios as well as between Poisson's ratios, deduced from the two data sets, are small. This was expected since for a layered medium and large epicentral distances (compared to focal depths), Wadati diagrams are mostly representative of Vp/Vs ratios in the deepest layer sampled by seismic waves (Lee and Steward, 1981).

STATION CORRECTIONS

We also examined whether or not the travel-time residuals, relative to the velocity model in Table 1, are azimuth dependent. In doing this, we used the formula

$$U_{ij} = A_j + B_j \sin(Z_{ij} + E_j) = A_j + C_j \sin(Z_{ij}) + D_j \cos(Z_{ij}) . \quad (5)$$

Where U_{ij} is the i-th residual at station j, Z_{ij} is the azimuth from source i to station j, and A_j , B_j and E_j are determined by the method of least-squares. A_j is called the mean station-correction, B_j is the amplitude and E_j is the phase of a sinusoidal function (Herrin and Taggart, 1968). Both the

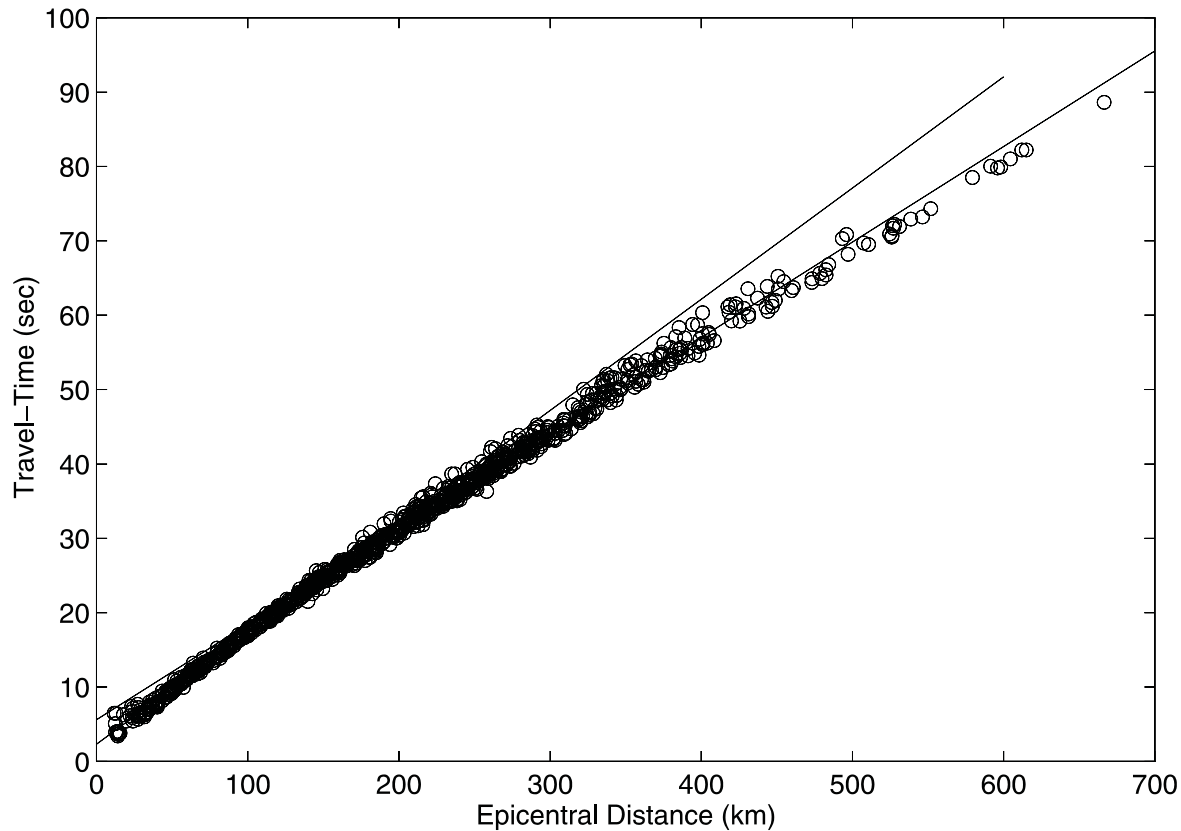


Fig. 4. Travel times of Pg and Pn waves versus epicentral distance. There are 994 measured travel times in the distance range from 11.6 km to 666 km used in the diagram.

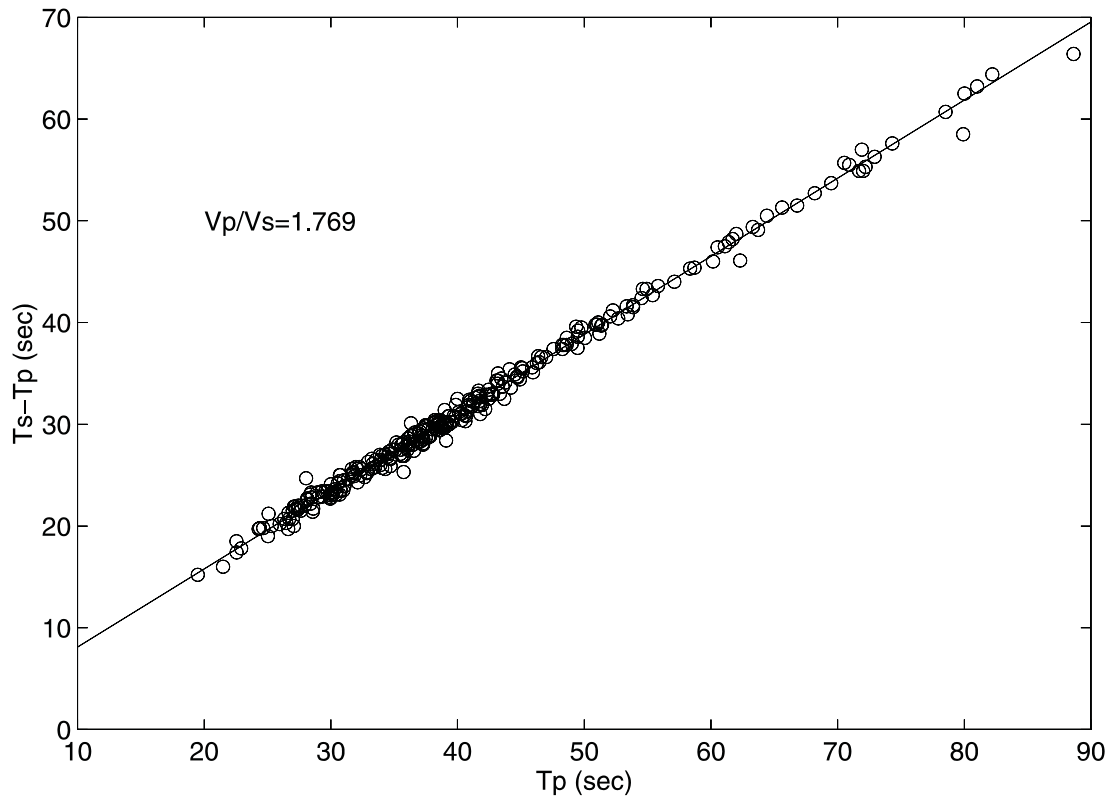


Fig. 5. Wadati diagram for 298 event-station pairs with recorded Pn and Sn waves. $V_p/V_s=1.769\pm 0.003$. Observe that travel times rather than arrival times are used in the diagram (see the text). Focal depth varies from 0 km to 45 km.

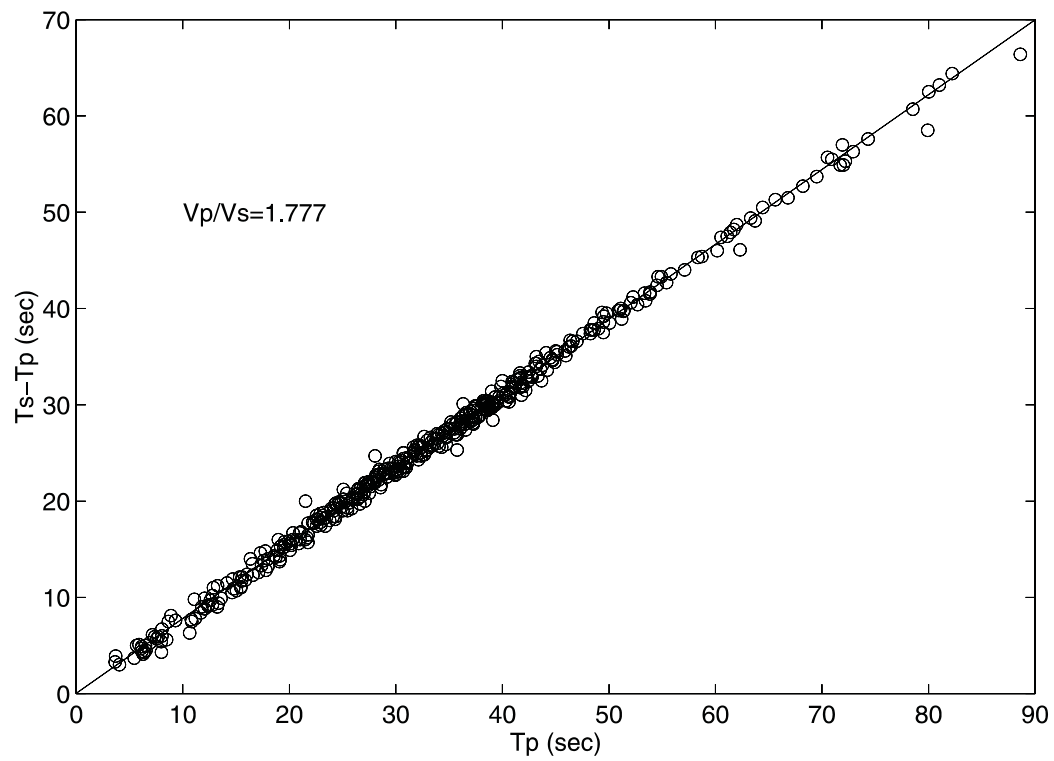


Fig. 6. Wadati diagram for events with focal depths between 0 and 45 km, showing a V_p/V_s value of 1.777 ± 0.002 , for 447 P and S wave travel times. Both direct (Pg, Sg) and refracted (Pn, Sn) waves are employed.

direct and refracted waves, i.e. P and Pn, respectively are included. If we assume no azimuthal effect, the station correction is the mean residual, $\frac{1}{N} \sum_{i=1}^N U_{ij}$, which needs to be calculated for each station.

As an example, Figure 7 shows the travel-time residuals without station correction, for station Cerro de la Muerte (CDM) with the highest altitude, plotted against azimuth. We found that the residuals at CDM for 92 events can be expressed as

$$U_{iCDM} = -0.15 + 0.12 \sin(Z_{iCDM} - 82.34^\circ) . \quad (6)$$

We repeated the procedure for 22 stations with 10 or more recorded events. Calculated station corrections are summarized in Table 2. Parameters A, B and E are the estimates of A_j , B_j and E_j , respectively, $j=1, \dots, 22$. N is the number of earthquakes considered, σ^2 is the variance of the regression

$$\sigma^2 = \left(\sum_{i=1}^N \frac{\epsilon_i^2}{(N-M)} \right) \text{ where } \epsilon_i \text{ is the residual } (T_{OBS} -$$

T_{CAL}) minus the “predicted” residual travel time (cf. eq. (5)), and M is the number of calculated parameters.

We repeated the analysis station by station, for the case when only Pn travel-time residuals were considered. In this case, the estimated standard errors for each station are large, i.e. of the same order as the estimated parameters A_j , B_j and E_j . One exception is the POA station, for which the least-squares method for 19 Pn travel-time residuals gives $A=0.15 \pm 0.05$, $B=0.47 \pm 0.12$ and $E=58.96^\circ \pm 3.16$ (Figure 8). These values indicate that for source-to-station azimuth approximately 30° and 210° , the POA station correction (Pn) is 0.6 sec too short and -0.3 sec, respectively. We believe that the high station corrections for TIG and VTU (Table 2) are associated with the local geology beneath these sites.

VELOCITY ANISOTROPY

To estimate the apparent velocity V_0 , time delays and to examine the possible variation of the Pn velocity as a function of azimuth, we employ the modified version of eq. (3) (Raitt *et al.*, 1969)

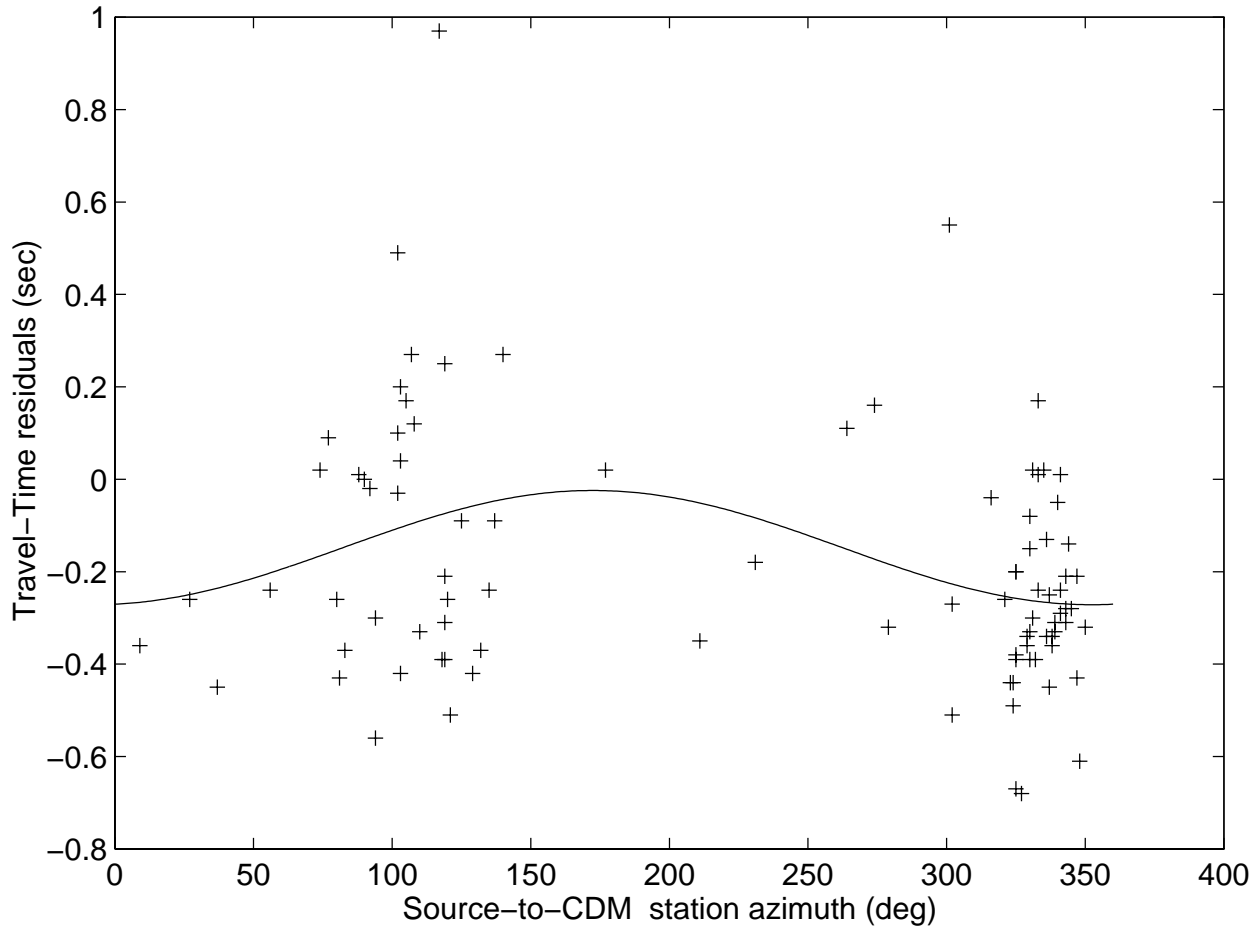


Fig. 7. 92 travel-time P-wave residuals measured at CDM station and plotted against source-to-station azimuth. The solid line is $U_i = A_i + B_i \sin(Z_i + E_i)$, eq. (5), where the residuals U_{iCDM} are relative to the 1D velocity model listed in Table 1, Z_{iCDM} is the azimuth from event i to station CDM, $A_i = -0.15$, $B_i = 0.12$ and $E_i = -82.34^\circ$.

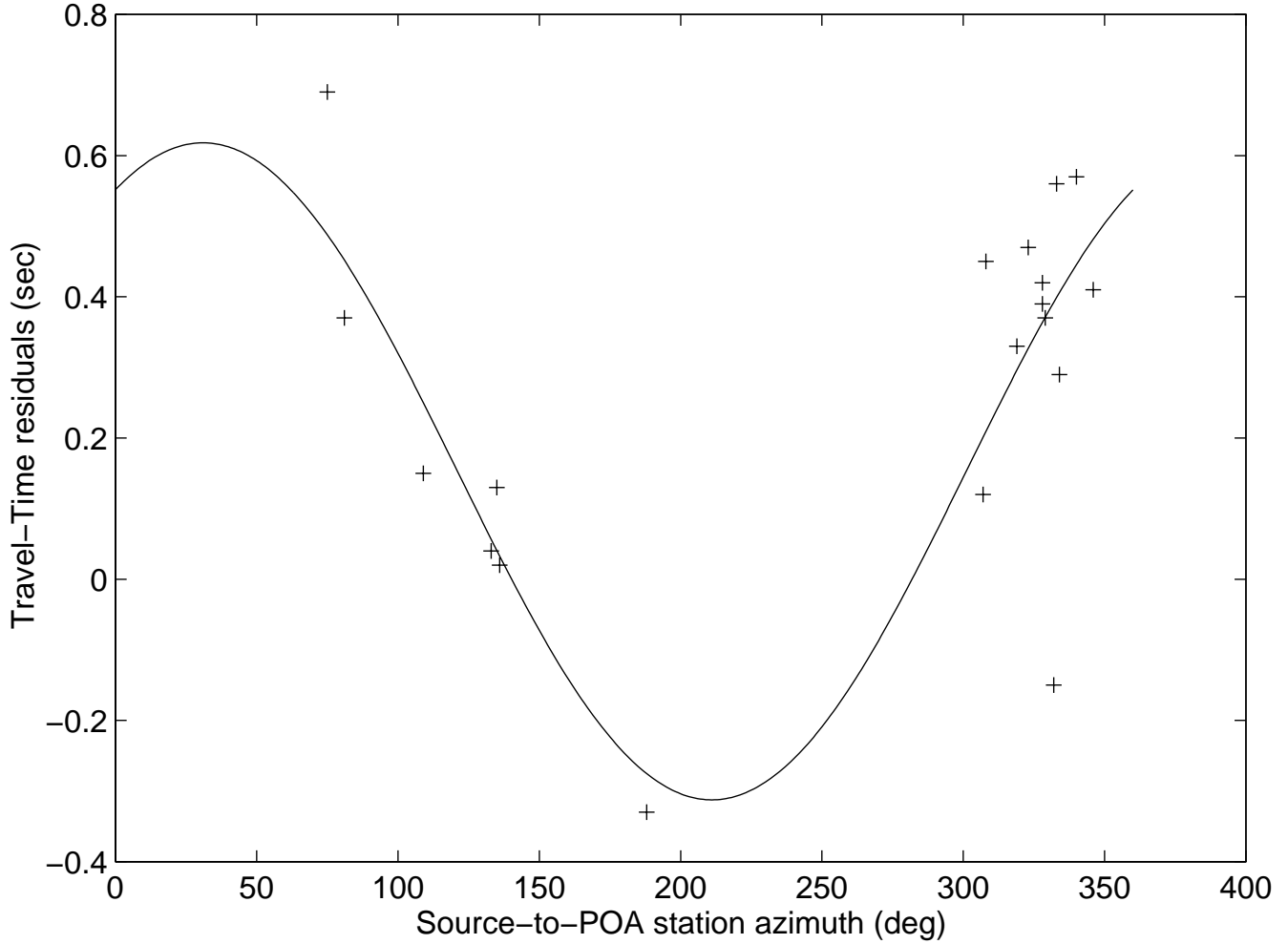


Fig. 8. Pn travel-time residuals for POA station plotted against source-to-station azimuth. The plotted curve is $U_i=A_i+B_i \sin(Z_i+E_i)$ according to eq. (5). The residuals U_i are relative to the 1D velocity model listed in Table 1, Z_i is the azimuth from event i to POA, $A_i=0.15$, $B_i=0.47$ and $E_i=58.96^\circ$. 19 Pn travel-times residuals were used.

$$t_{ij} = a_i+a_j+\Delta_{ij}/V_0+(Fa+Fb-\Delta_{ij})/ V_0^2 \delta v \quad (7)$$

where t_{ij} is the travel time from source i to receiver j , a_i and a_j are time delays at the source and receiver, respectively, Fa and Fb are horizontal offsets between the source and receiver and the point of critical refraction, respectively, and δv represents a weak anisotropy of the Pn refractor velocity. Note that the approach based on eqs. (7) does not require a specific initial velocity model, which was the case in the preceding section. An offset distance could be used instead Fa and Fb (Morris *et al.*, 1969). By solving a set of eqs. (7) we inverted simultaneously for V_0 , δv , a_i , a_j . Whereas eq. (5) is solved for one station at a time, eqs. (7) are inverted for all stations at the same time.

Backus (1965) shows that small anisotropy can be represented in the form

$$\delta v = A \cos 2\phi + B \sin 2\phi + C \cos 4\phi + D \sin 4\phi \quad (8)$$

where the parameters A , B , C , D are functions of the anisotropic elasticity of the upper mantle and ϕ is the source-to-receiver azimuth.

The velocity variation between any source-station pair is estimated using eq. (7), i.e.

$$\delta v = (t_{ij} - a_i - a_j - \Delta_{ij}/V_0) V_0^2 / (Fa+Fb-\Delta_{ij}) \quad (9)$$

The estimated velocities are plotted in Figure 9 as a function of angle ϕ . The solid line in the figure represents the calculated velocity using 2ϕ and 4ϕ terms of the Backus anisotropy function specified by eq. (8).

To solve eq. (7), we arbitrarily fix the time term of one selected station and the other delay times are calculated relative to the fixed one, as defined in McCollom and Crosson (1975). Table 3 summarizes the results for least-squares analyses that use 571 arrivals from 94 earthquakes, recorded at 23

Table 2

Calculated station corrections *

Station	N	A±σ	B±σ	T±σ	σ ²
IRZ2	86	0.06±0.058	0.06±0.03	-71.24±90.37	0.073
POA	22	0.09±0.058	0.50±0.15	58.16±3.57	0.053
POA2	51	0.15±0.084	0.05±0.135	71.44±10.28	0.067
QPS	80	0.12±0.039	0.28±0.07	260.32±3.7	0.106
CDM	92	-0.15±0.036	0.12±0.03	-82.34±39.44	0.067
EPA	86	0.11±0.044	0.15±0.07	202.31±42.86	0.104
PTCR	83	-0.11±0.030	0.09±0.06	11.04±16.35	0.06
HDC2	80	0.19±0.055	0.13±0.09	77.38±10.11	0.076
HDC	11	0.14±0.188	0.21±0.51	66.3±13.29	0.059
CAO	83	-0.11±0.038	0.12±0.1	227.57±16.0	0.10
JUD	64	0.08±0.038	0.16±0.093	63.60±3.97	0.083
RIN	10	-0.16±0.098	0.09±0.026	258.45±104.5	0.055
RIN2	12	0.06±0.20	0.24±0.104	185.9±69.74	0.03
RIN3	22	-0.01±0.107	0.20±0.093	204.5±81.37	0.068
PBC	58	0.05±0.065	0.13±0.024	-81.36±74.18	0.210
CTCR	20	-0.30±0.169	0.32±0.093	-80.33±59.46	0.261
VACR	13	0.23±0.272	0.19±0.465	87.12±24.95	0.237
IDC	25	0.06±0.064	0.31±0.133	226.9±7.55	0.055
JTS	34	0.02±0.134	0.32±0.212	218.4±48.34	0.182
TIG	18	0.49±0.092	0.55±0.142	262.55±7.51	0.117
VTU	14	-0.75±0.454	1.05±0.565	59.00±0.97	0.025
OCM	21	-0.30±0.081	0.21±0.116	99.10±3.0	0.028

* N = number of earthquakes.

A, B, E = coefficients in eq. (5)

σ² = variance (see the text)

Stations with 9 or less observations are not included

stations. The CDM station delay was fixed at 1 sec, and the other delay times are calculated relative to the CDM delay. The standard error about the regression is equal to 0.32 sec, the mean velocity is 7.81 km/sec, and the magnitude of the 2ϕ and 4ϕ terms is 0.078 km/sec and 0.053 km/sec, respectively. The magnitude of the 2ϕ (4ϕ) term is computed by taking the square root of the sum of squares of A and B (C and D) coefficients (Morris *et al.*, 1969). Numerical results are summarized in Table 4. For the case $t_{ij} = a_i + a_j + \frac{\Delta_{ij}}{V_p}$, i.e. no azimuthal velocity dependence, the Pn velocity is similar to that deduced from the diagram in Figure 3. Hence, we conclude that the present data do not indicate any significant anisotropy of the Pn velocity. For more conclusive results

one would obviously need a data set with more even distribution of source-to-station azimuths (cf. Figure 2).

CONCLUSIONS

Travel-time analyses of 100 regional earthquakes, recorded by the OVSICORI-UNA seismographic network with an assumed multilayered velocity model show the following:

Poisson's ratio for the uppermost mantle beneath Costa Rica is $\sigma = 0.265$. The best linear fit for the direct and refracted wave gives the velocity ratio $V_p/V_s = 1.78$.

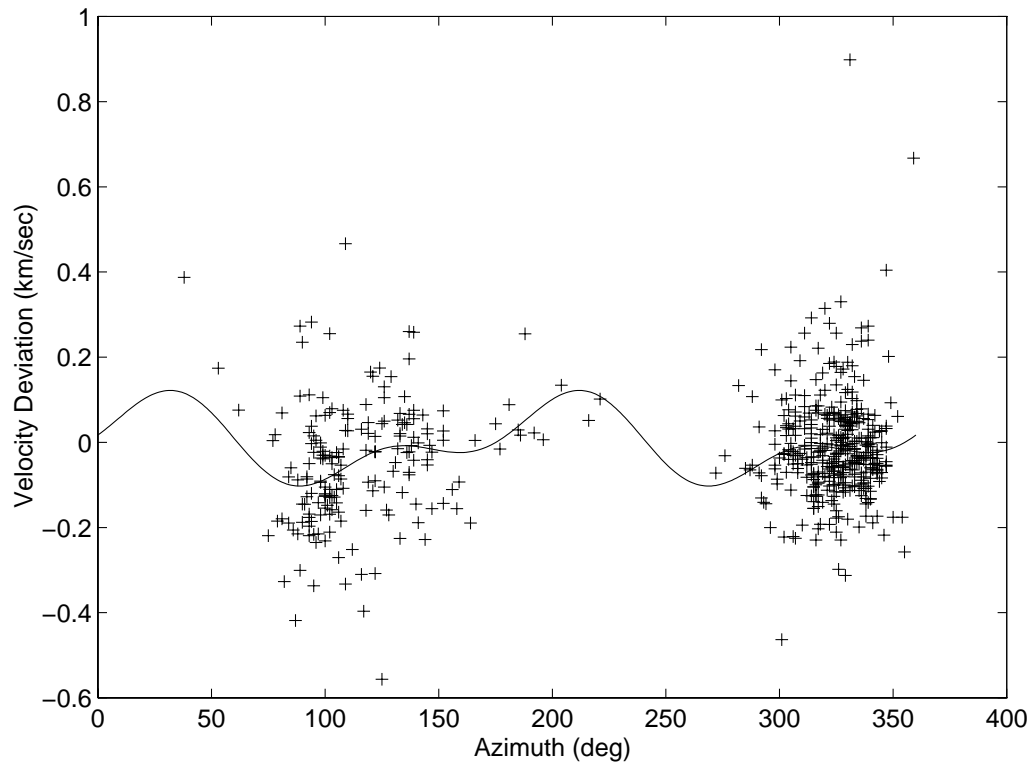


Fig. 9. Pn-velocity anisotropy expressed as deviation from mean velocity of 7.81 km/sec, plotted as a function of azimuth. The solid line represents Pn velocity deviation calculated from eq. (8). The deduced parameters are $A=0.061$, $B=0.049$, $C=-0.043$, $D=0.031$. The B and C terms are small when compared with their standard errors. Data in the figure are from the 100 events and stations shown in Figure 1. The largest anisotropy term, $\sqrt{A^2 + B^2}$ is 0.078 km/sec. The other term, $\sqrt{C^2 + D^2}$ is 0.053 km/s and close to the standard deviation.

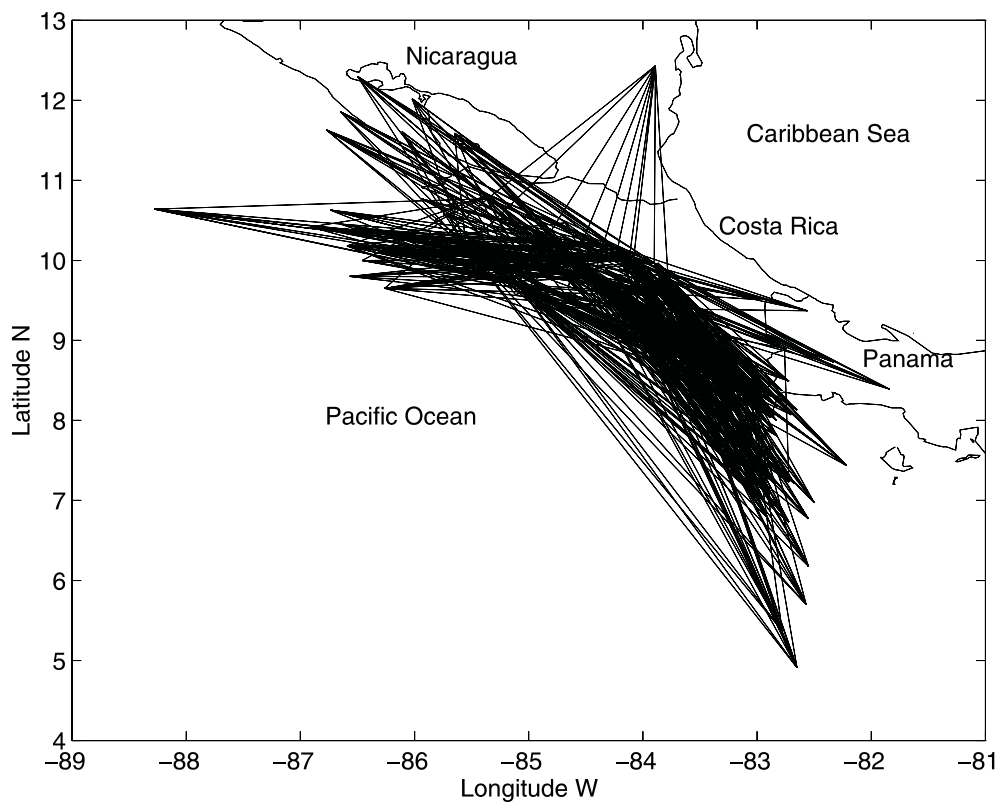


Fig. 10. Source-to-station pairs employed in the present study.

Table 3

Station delay-times obtained according to eq. (7)*)

Station Code	Station Delay Time (sec)	Standard errors (sec)	Station delay with elevation correction (sec)
CDM	1.000	Reference	1.000
IREZ	0.275	0.055	1.273
IRZ2	1.141	0.091	1.236
POA	1.202	0.064	1.472
POA2	1.189	0.081	1.380
QPS	0.462	0.065	1.126
EPA	0.706	0.084	1.326
PTCR	0.677	0.094	1.061
HDC	0.880	0.125	1.333
HDC2	0.967	0.065	1.409
CAO	0.382	0.071	1.012
EUD	0.671	0.084	1.186
RIN	0.741	0.169	1.269
RIN2	0.812	0.177	1.218
RIN3	0.599	0.161	1.093
PRC	0.790	0.128	1.442
CTCR	0.635	0.189	0.995
VACR	1.365	0.225	1.975
JIX	0.693	0.133	1.373
JIS	0.542	0.103	1.156
TRG	0.836	0.152	1.381
OCM	0.677	0.159	1.032
CVT	0.550	0.340	0.740

*) We correct for the elevation according to the formula $c=(3.47\text{-altitude})/5.1$, where 3.47 km is the CDM altitude. The value is added to the second column and the result is given in the fourth column.

Table 4

Anisotropy results

Coefficients eqs (7,8)	Numerical values km/sec	Standard errors km/sec
Vo	7.81	0.030
A	0.061	0.031
B	0.049	0.037
C	-0.043	0.018
D	0.031	0.024

The Pn velocity obtained in this study is 7.81 km/sec, which is in good agreement with the Pn velocity found by Matumoto *et al.*, (1977).

The Pn velocity deduced for an assumed isotropic material is close to the velocity for an anisotropic case. We conclude that the present data (with highly uneven azimuthal distribution) do not indicate any significant anisotropy of the Pn velocity.

Pn travel-time residuals do not give any evidence of azimuth dependence, with the exception of the POA station (Figure 8). In general, if the residuals do not show azimuthal effect, the station correction for each station can be found through the mean of the residuals (Table 2).

The calculated Moho depth beneath Costa Rica is about 34 km, which differs from that of 43 km presented by Matumoto *et al.* (1977). The latter is derived from observations made by a 25km x 25km array (except one outlier station) around the Arenal volcano in northern Costa Rica. Their result is, therefore, relevant only for a rather limited area of the country.

In contrast, source-to-station pairs employed in this study (Figure 10), sample crust and the upper mantle beneath the entire Costa Rica, except a narrow strip along the Caribbean coast, and consequently provide an average Moho thickness for the whole country. Our Moho depth is in good agreement with those available for Japan, Mexico and South America (Matumoto *et al.*, 1977) i.e. 33, 38 and 29 km, respectively, whereas the thickness given by Matumoto *et al.*, (1977) for Costa Rica appears to be too large. Also, Fan *et al.*, (1990) estimated the crustal thickness in southeastern Costa Rica to lie between 28 km and 35 km. For northern Central America (Honduras), Kim *et al.*, (1982) give an average crustal thickness of 37.4 km. These results again are in agreement with that found in this study.

ACKNOWLEDGMENTS

This work was carried out at the Department of Earth Sciences, Seismology, Uppsala University, Sweden, as a part of the SERCA/SAREC project. The Swedish Agency for Research Cooperation (SAREC) and the Universidad Nacional de Costa Rica (UNA) provided financial support.

BIBLIOGRAPHY

BACKUS, G. E., 1965. Possible forms of seismic anisotropy of the uppermost mantle under oceans. *J. Geophys. Res.*, 70, 3429-3439.

FAN, G., S. L. BECK and T. C. WALLACE, 1993. The Seismic Source Parameters of the 1991 Costa Rica Aftershock Sequence: Evidence for a Transcurrent Plate Boundary. *J. Geophys. Res.*, 98, 15,759-15,778.

GÜENDEL, F. D., 1986. Seismotectonics of Costa Rica: An analytical view of the Southern Terminus of the Middle

- America Trench. Ph.D. Thesis, University of California, Santa Cruz.
- GÜENDEL, F., K. C. MCNALLY, J. LOWER, M. PROTTI, R. SAENZ, E. MALAVASSI, J. BARQUERO, R. VANDER LAAT, V. GONZALES, C. MONTERO, E. FERNANDEZ, D. ROJAS, J. D. D. SEGURA, A. MATA and Y. SOLIS, 1989. First results from a new seismographic network in Costa Rica, Central America. *Bull. Seism. Soc. Am.*, 79, 205-210.
- HERRIN, E. and J. TAGGART, 1968. Regional Variation in P Travel times. *Bull. Seism. Soc. Am.*, 58, 4, 1325-1337.
- KIM, J. J., T. MATUMOTO and G. V. LATHAM, 1982. A crustal section of northern Central America as inferred from wide-angle reflections from shallow earthquakes. *Bull. Seism. Soc. Am.*, 72, 925-940.
- KISSLINGER, C. and E. R. ENGDAHL, 1973. The interpretation of the Wadati Diagram with relaxed assumptions. *Bull. Seism. Soc. Am.*, 63, 1723-1736.
- KLEIN, F. W., 1984. User's guide to Hypoinverse, a program for Vax and Pc350 computers to solve for earthquake locations, U. S. Geological Survey, Open File Report 84-000.
- LEE, W. H. K. and S. W. STEWART, 1981. Principles and Applications of Microearthquake Networks. Academic Press, New York, 293 pp.
- MANN, P., 1995. Preface. In: Mann, P. (ed.), Geologic and Tectonic Development of the Caribbean Plate Boundary in Southern Central America: Boulder, Colorado, Geological Society of America, Special Paper.
- MATUMOTO, T., M. OHTAKE, G. LATHAM and J. UMAÑA, 1977. Crustal structure in southern Central America. *Bull. Seism. Soc. Am.*, 67, 121-134.
- MORRIS, G. B., R. W. RAITT and G. G. SHOR, 1969. Velocity anisotropy and delay-time maps of the mantle near Hawaii. *J. Geophys. Res.*, 74, 4300-4316.
- McCOLLUM, R. L. and R. S. CROSSON, 1975. An array study of upper mantle velocity in Washington State. *Bull. Seism. Soc. Am.*, 65, 467-482.
- OVSICORI, HEREDIA, 1993. Costa Rica. Catálogo de Temblores, 1989, 170 pp.
- RAITT, R. W., G. G. SHOR, T. J. G. FRANCIS and G. B. MORRIS, 1969. Anisotropy of the Pacific upper mantle. *J. Geophys. Res.*, 74, 3095-3109.
- SILVER, E. A., J. GALEWSKY and K.D. McINTOSH, 1995. Variation in Structure, Style, and Driving Mechanism of Adjoining Segments of the North Panama deformed belt. In: Mann, P. (ed.), Geologic and Tectonic Development of the Caribbean Plate Boundary in Southern Central America. Boulder, Colorado, Geological Society of America, Special Paper, pp. 225-233.
- SCHEIDEGGER, A. E. and P. L. WILLMORE, 1957. The use of a least squares method for the interpretation of data from seismic surveys. *Geophysics*, 22, 9-22.

Ronnie Quintero^{1,2} and Ota Kulhanek²

¹ Observatorio Vulcanológico y Sismológico de Costa Rica, Heredia, Costa Rica. E-mail: rq@geofys.uu.se

² Department of Earth Sciences, Seismology, Uppsala University, Sweden. E-mail: Ota.Kulhanek@seismo.uu.se